Chalcogenide Letters Vol. 15, No. 8, August 2018, p. 405 - 410

PREPARATION AND ADSORPTION CAPABILITY OF ZnSe HOLLOW NANOSPHERES

J. J. LIU, M. Q. XUE*
Changzhou Vocational Institute of Light Industry, Changzhou, Jiangsu 213164, P. R. China

A facile method for a direct synthesis of the stable and crystalline phase pure ZnSe hollow nanospheres was developed using by a hydrothermal and calcination process. X-ray diffraction (XRD) analysis, energy-dispersive spectroscopy (EDS), scanning electron microscopy (SEM) and nitrogen adsorption-desorption measurements were used to examine the morphology and the microstructure of the obtained compound. The morphological study clearly revealed that the as-prepared ZnSe nanospheres have a diameter of around 1μm and are hollow structures with shell thickness of about 10 nm which are constructed by numerous nanocrystals. The adsorption properties of ZnSe hollow nanospheres were tested by the adsorption of methylene blue (MB). The results show an excellent removal capacity for organic pollutant MB from the waste water, making them a promising candidate for waste water treatment.

(Received May 22, 2018; Accepted August 3, 2018)

Keywords: ZnSe, Hollow nanospheres, Hydrothermal and calcination process

1. Introduction

Hollow micro-/nanostructures are of great interest in many fields of application and areas of technology. For example, hierarchical SnO_2 hollow nanostructures manifested high capacities and excellent cycle performances as the anode materials for lithium ion batteries [1], ellipsoidal hollow nanostructures TiO_2 used as a magnetically separable photocatalyst [2], hierarchical hollow nanostructures MnO_2 combined with novel chemical and physical properties used in water treatment, the hollow nanostructures CuO exhibited excellent electrochemical performance for lithium-ion batteries[4]. Likewise, metal sulfide hollow nanostructures used as electrode materials for electrical energy storage systems due to their unique structural features and rich chemistry [5-6].

Thus, it is of great interests to synthesize nanocrystals with a hollow nanostructure. Up to now, various methods have been employed to obtain hollow nanostructures. Li et al. prepared TiO_2 hollow spheres through a facile hydrothermal route [7]. Singh et al. synthesized copper (II) oxide hollow nanostructures by applying the soft templating effect provided by the confinement of droplets in miniemulsion systems [8]. Kang et al. prepared $ZnGa_2O_4$ hollow nanostructures by a two step hydrothermal and calcination process using carbon spheres as a template [9]. Zhou et al. reported a dissolution-recrystallization process to prepared Fe_2O_3 hollow nanostructures [10]. Yang et al. prepared $Co(OH)_2$ hollow nanostructures including cube, octahedron and flower using one-step Cu_2O template etching method [11]. Among these methods, the complex operation is a negative factor to achieve the final hollow nanostructures. Therefore, a simple, effective and economical method is strongly desired to synthesize hollow nanospheres.

As an important II–VI semiconductor, ZnSe is probably one of the most important electronic and optoelectronic materials, which offer its promising applications in nonlinear optical devices, flat panel displays, light emitting diodes, lasers, logic gates, transistors, etc [12] .

At present, several attempts have been made in the syntheses and properties of ZnSe hollow spheres. Geng et al. [13] generated ZnSe hollow microspheres by a simple chemistry vapor deposition method in a horizontal tube furnace, and found that the hollow ZnSe microspheres exhibit strong blue emissions with the intensities being adjustable. Wei et al. [14] fabricated

*Corresponding author: xuemaoq@163.com

micro-sized hollow spheres of cubic ZnSe through two-sourced evaporation method in a quartz tube at 410°C. Liu et al. [15] produced ZnSe hollow nanospheres with bubble templating through a facile one-pot hydrothermal method, the ZnSe hollow nanospheres were exhibited adsorption maxima at 278 and 426 nm, which have promising applications in blue emitters, catalysts, and gas sensors. Meanwhile, ZnSe hollow spheres were successfully synthesized via simple hydrothermal method with CTAB as the soft template [16-17]. Hollow-sphere ZnSe is successfully obtained through Ostwald ripening [18].

The template methods mentioned above are complicated, time-consuming, and often break the hollow sphere during template removal. chemistry vapor deposition and evaporation method require high energy consumption and certain equipment requirements, which lead to energy and time consuming, complicated productive process and low production efficiency. The hydrothermal method is relatively simple and convenient, which can be easily control the phase and morphology of the resultant products by adjusting the synthesis conditions including solvents, ion concentration temperature, pH value, duration, etc.

In this paper, we successfully fabricated ZnSe hollow nanospheres by utilizing a facile hydrothermal method. This synthetic approach is simple, effective, low cost and environmentally friendly. Then, the as-prepared ZnSe hollow nanospheres were analysed using XRD, SEM, EDS and BET, and the adsorption capability of the ZnSe hollow nanospheres on methylene blue removal were investigated.

2. Experimental

2.1 Synthesis of ZnSe hollow nanospheres

All reagents (analytical-grade purity) were used without any further purification. In a typical synthesis, 1 g zinc acetate dehydrate ($C_4H_6O_4Zn{\cdot}2H_2O$), 0.4 g Se powder and 5 g Polyvinyl pyrrolidone (PVP) were dissolved in a mixture of ethylene glycol (58 ml) and distilled water (10 ml). After stirring for 30 min, the above solution was transferred into a Teflon-lined stainless steel autoclave, sealed tightly, and maintained at 200 °C for 48 h. After the autoclave was cooled down to room temperature naturally, the precipitates were washed with deionized water and absolute ethanol for several times using a centrifuge, and then dried at 70 °C for 12 h. The precipitates were calcined at 500 °C for 2 h with a heating rate of 5 °C/min. The calcined products were then collected for further analysis.

2.2 Characterization

X-Ray power diffraction (XRD) analysis was conducted on a D8 advance (Bruker-AXS) diffractometer with Cu Ka radiation (λ=0.1546 nm) in the range of 10–80°, data analysis with Jade software. The composition was characterised by energy-dispersive spectroscopy (EDS). The morphologies and structures of the samples was examined by field-emission scanning electron microscopy (FESEM, SEM, JEOL JXA-840A, operated at an acceleration voltage of 15 kV) equipped with single crystal W cathode. The samples for the SEM and EDS studies were prepared by placing the ZnSe powders on to a copper disk with conducting resin followed by metal spraying. Specific surface areas and pore parameters of the samples were measured at 77 K by Brunauer–Emmett–Teller (BET) nitrogen adsorption–desorption (Autosorb-iQ2-MP, Quanthachrome, USA).

2.3 Adsorption experiment

The adsorption performances of the ZnSe hollow nanospheres were evaluated by removing methylene blue (MB) from aqueous solution. Typically, 0.025 g of powders was added into 40 mL of MB solution (20 mg/L). The suspension was stirred for 360 min to reach an adsorption–desorption equilibrium of dye molecules on the solid surface. During adsorption process, 3 mL of suspension was collected at a given time interval and centrifuged to remove the adsorbent. The concentration of dye remaining in the solution was determined by UV-Vis spectrophotometry. All the adsorption tests were kept at room temperature without adjusting pH of dye solution.

3. Results and discussions

The crystallinity, structure, and phase purity of the prepared samples were confirmed by XRD and EDS. Fig. 1a shows the XRD pattern of the ZnSe sample fabricated by the hydrothermal reaction $C_4H_6O_4Zn{\cdot}2H_2O$, PVP and Se powder in mixture of ethylene glycol and distilled water at 200 ^oC for 48 h.

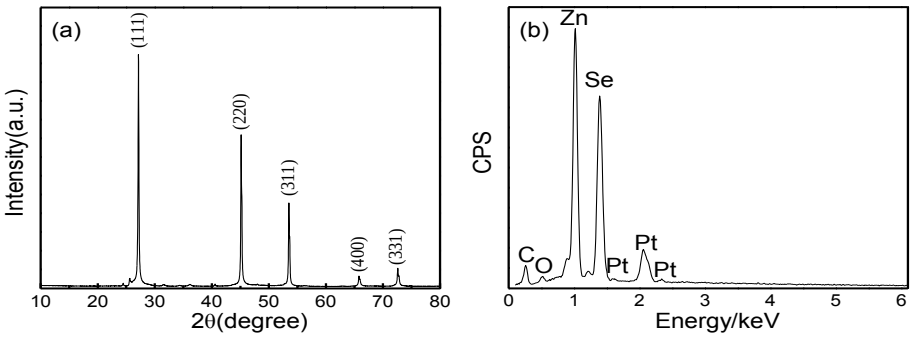

Fig. 1. (a) XRD pattern and (b) EDS of the as-prepared ZnSe.

All peaks in the XRD pattern can be readily indexed to the cubic (F-43m space group) ZnSe phase, with lattice constants a=5.669Å, which are in good agreement with the reported values (JCPDS card no.37-1463). No characteristic peaks from other impurities are observed in the XRD pattern, indicating the high purity of the $MoSe_2$ samples. Energy-dispersive spectrometer (EDS) result as shown in Fig. 1b reveals that the sample consisted of element Zn and Se, the quantification of the peaks shows that the atom ratio between Mo and Se is about 1.33:1, which is close to the stoichiometric ZnSe.

The morphology of the obtained ZnSe products was investigated by SEM. Fig. 2a displayed the low magnification SEM images of ZnSe nanomaterials, these nanomaterials composed of many particles.

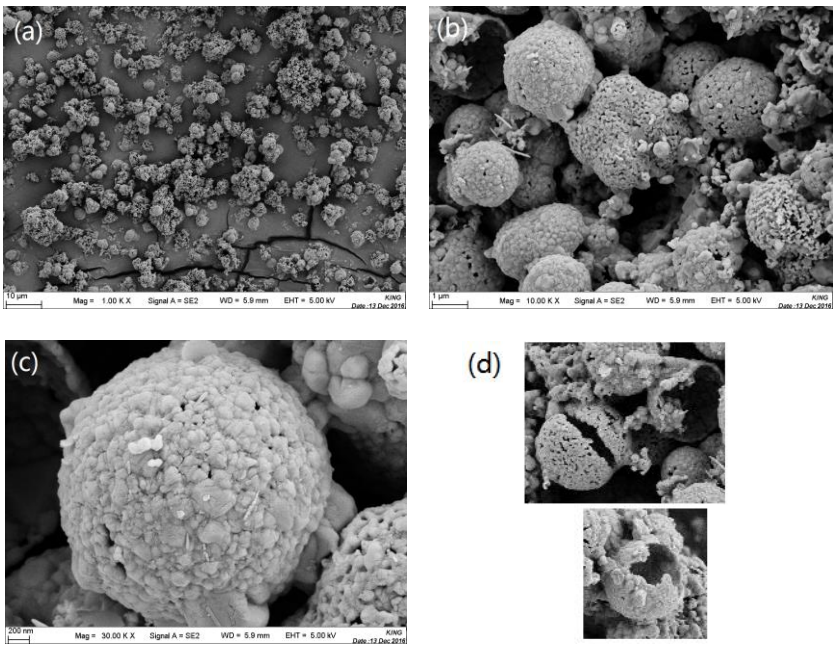

Fig.2. SEM image of the ZnSe hollow nanospheres.

An enlarged SEM image apparently showed that the obtained samples mainly comprised of nanospheres, as shown in Fig. 2b. Further insight into the morphology and microstructure of ZnSe nanomaterials as shown in Fig. 2c, the diameter of the as-synthesized ZnSe nanospheres was about 1μm. The high- magnification image of the nanospheres were hollow in structure as shown in Fig. 2d. It has been found that the wall thickness was about 10 nm.

Nitrogen adsorption experiment was performed to evaluate the porosity and surface area of the as-synthesized hollow nanospheres structures. The nitrogen adsorption and desorption isotherm plots and corresponding pore-size distribution plots of the ZnSe hollow nanospheres are given in Fig.3.

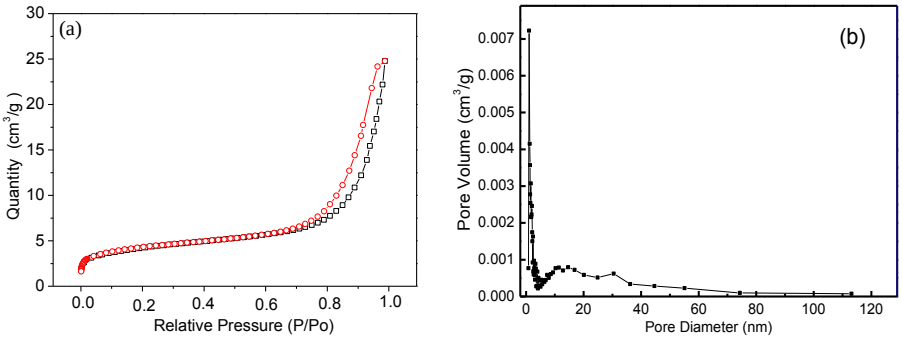

Fig. 3 Nitrogen adsorption–desorption isotherm and corresponding pore-size distribution of as-synthesized ZnSe hollow nanospheres.

The nitrogen adsorption–desorption isotherm of ZnSe hollow nanospheres in Fig.3a exhibits characteristics of type IV according to the classification of the International Union of Pure and Applied Chemistry, the hysteresis loop at high relative pressure indicates the presence of mesopores. The BET surface area of the product was calculated to be 14.3167 m^2g^{-1}. From the curves in Fig.3b, we can see that this sample has an obvious peak in the pore-size distribution plot at about 1.1 nm, and displays porous structures with a wide range of pore size distributions from 1.0 nm to 113 nm, which will provide more surface active sites and pore channels for the adsorption and diffusion of dyes, thus improving the adsorption performance [19].

The adsorption activities of ZnSe hollow nanospheres were evaluated by the degradation of MB in aqueous solution. Fig. 4 a presents the effect of contact time on the adsorption capacity of MB of the prepared ZnSe hollow nanospheres.

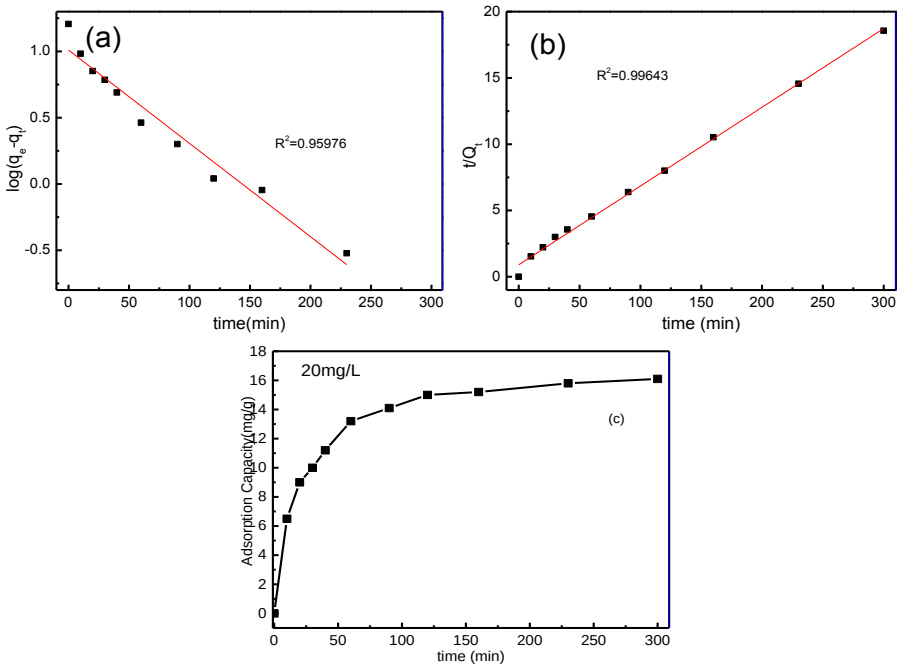

Fig. 4. The adsorption curves of MB of the prepared ZnSe hollow nanospheres
(a) effect of contact time on adsorption; (b) pseudo-first-order; (c) pseudo-second-order.

It was observed that the adsorption capacity of MB increased with increasing contact time. The adsorption process had two stages: the adsorption behavior at the initial stage was rapid; the adsorption behavior at the second stage was very slow and it took 180 min. to achieve adsorption equilibrium state.

To evaluate the absorption kinetics of MB of the prepared ZnSe hollow nanospheres, the two kinetics models including the pseudo-first-order kinetic model and the pseudo-second-order kinetic model were used to analyze obtained experimental data. The pseudo-first-order and pseudo-second-order kinetic models were expressed by Eqs. (1) and (2):

$$\log(q_e - q_t) = \log q_e - \frac{k_1 t}{2.303} \tag{1}$$

$$\frac{t}{q_t} = \frac{1}{k_2 q_e^2} + \frac{t}{q_t} \tag{2}$$

where q_e (mg/g) and q_t (mg/g) are the adsorption capacity of ZnSe hollow nanospheres at equilibrium state and at time t (min.), respectively; k_1 (min^{-1}) and k_2 [g/(mg·min)] is the rate constants of the pseudo-first-order kinetic model and the pseudo-second-order kinetic model, respectively.

The pseudo-first-order curves of MB over samples are shown in Fig. 4b. The plots of t/Q_t versus t (pseudo-second-order curves) are shown in Fig. 4c, the correlation regression coefficient (R^2= 0.99643) of the pseudo-second-order kinetic model was greater than that (R^2= 0.95976) of the pseudo-first-order kinetic model, which indicates that the pseudo-second-order kinetic model is suitable for describing the adsorption process. This result implied that the adsorption process was mainly controlled by chemisorptions, rather than by physical adsorption [20-22].

4. Conclusions

In summary, the novel ZnSe hollow nanospheres have been successfully synthesized by a facile hydrothermal method. The approach provided a simple, effective, low-cost, and environment friendly method to synthesize the ZnSe hollow nanospheres. The prepared ZnSe hollow nanospheres with a porous structure and exhibited excellent wastewater treatment performance with high removal capacities to organic dyes.

The adsorption experiments indicated that the ZnSe hollow nanospheres exhibit outstanding adsorption capacity for methylene blue in aqueous solution. Owing to their outstanding adsorption capacity, the ZnSe hollow nanospheres were promising candidates for environmental applications.

Acknowledgments

This work was supported by the Innovation Training Programs for Undergraduates of Jiangsu Province (201813101002Y), 333 Project of Jiangsu Province and Qinglan Project of Jiangsu Province.

References

[1] X. M. Yin, C. C. Li, M. Zhang, The Journal of Physical Chemistry C **114**, 17 (2010).
[2] J. S. Chen, C. Chen, J. Liu, Chemical Communications **47**, 9 (2011).
[3] J. B. Fei, Y. Cui, X. H. Yan, Advanced Materials **20**, 3 (2008).
[4] D. Ji, H. Zhou, Y. Tong, Chemical Engineering Journal **313**, (2017).
[5] X. Y. Yu, L. Yu, X. W. D. Lou, Advanced Energy Materials **6**, 3 (2016).
[6] X. Y. Yu, L. Yu, X. W. D. Lou, Small Methods **1**, 1 (2017).
[7] Y. Li, J. Luo, X. Hu, Journal of Alloys and Compounds **651**,(2015).
[8] I. Singh, K. Landfester, A. Chandra, Nanoscale **7**, 45 (2015).
[9] B. K. Kang, H. D. Lim, S. R. Mang, Cryst. Eng. Comm. **17**, 11 (2015).
[10] K. Zhou, Y. Zhen, Z. Hong, Materials Letters **190**, (2017).
[11] H. Yang, J. Xie, S. Juan Bao, Journal of colloid and interface science **457**, (2015),.
[12] Q. Zhang, H. Li, Y. Ma, Progress in Materials Science **83**, (2016).
[13] B. Geng, J. You, F. Zhan, J. Phys. Chem. C **112**, 112 (2008).
[14] J. Wei, K. Li, J. Chen, Journal of Alloys & Compounds **531**, 32 (2012).
[15] X. Liu, J. Ma, P. Peng, Langmuir the Acs Journal of Surfaces & Colloids **26**, 12 (2010).
[16] Y. X. Yang, C. J. Tang, Q. Niu, Journal of Henan University of Science & Technology **55**, 11 (2011).
[17] H. Wang, F. Du, Crystal Research & Technology **41**, 4 (2010).
[18] Z. Wang, X. Cao, P. Ge, New Journal of Chemistry **41**, 14 (2017).
[19] F. Xu, Z. Tang, S. Huang, Nature Communications **6**, (2015).
[20] H. J. Song, S. You, X. H. Jia, Applied Physics A **121**, 2 (2015).
[21] X. F. Sun, B. Liu, Z. Jing, Carbohydrate Polymers **118**, (2015).
[22] L. Zhang, Y. Liu, S. Wang, Rsc. Advances **5**, 121 (2015).